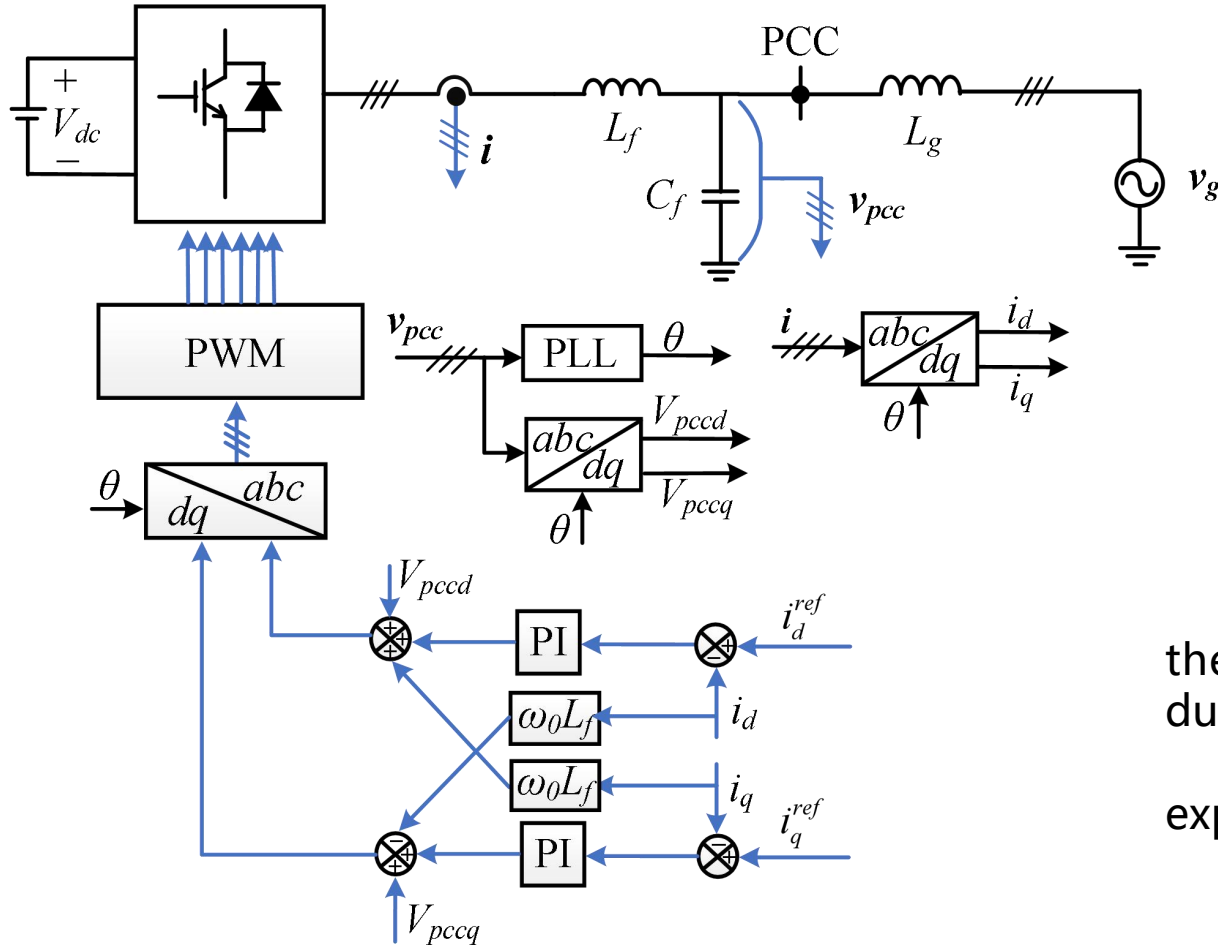


Instability Analysis of Grid-Connected Inverters During Low-voltage-ride Through Process

Cheng Luo, TBEA Xi'an Electric Technology Co.

System Description



$$I_d^{ref} = \begin{cases} I_{rate} & 0.9\text{p.u.} \leq V_{pcc} \leq 1.1\text{p.u.} \\ (0.2 \sim 0.4) * I_{rate} & V_{pcc} < 0.9\text{p.u.} \end{cases} \quad (1)$$

$$I_q^{ref} = \begin{cases} 0 & 0.9\text{p.u.} \leq V_{pcc} \leq 1.1\text{p.u.} \\ k_{q_adj} * (0.9 - V_{pcc}) * I_{rate} & V_{pcc} < 0.9\text{p.u.} \end{cases} \quad (2)$$

The grid code requires that the inverters need to raise the PCC voltage by injecting reactive current into the grid during LVRT process.

It is found that under this circumstance, the system may experience instability, especially under the weak grid.

Fig.1 System diagram of grid-connected inverters.

Problem Description

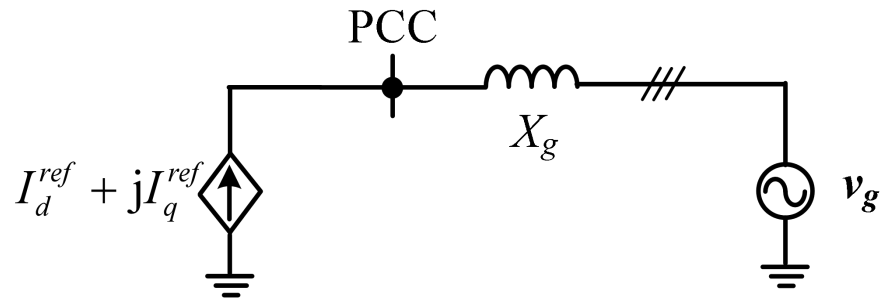


Fig. 2 Simplified diagram of the system.

$$V_{pcc} = V_g e^{-j\delta} + (I_d^{ref} + jI_q^{ref}) \cdot jX_g$$

⇓

$$V_{pccd} = V_g \cos(\delta) - I_q^{ref} X_g \quad (3)$$

$$V_{pccq} = -V_g \sin(\delta) + I_d^{ref} X_g$$

↓

$$V_{pcc} = V_{pccd} = \sqrt{V_g^2 - (I_d^{ref} X_g)^2} - I_q^{ref} X_g \quad (4)$$

↓

$$V_{pcc}(n+1) = \sqrt{V_g^2 - (I_d^{ref} X_g)^2} + k_{q_adj} (0.9 - V_{pcc}(n)) X_g \quad (5)$$

Problem Description

$$V_{pcc}^* = \frac{\sqrt{V_g^2 - (I_d^{ref} X_g)^2} + 0.9k_{q_adj} X_g}{1 + k_{q_adj} X_g} \quad (6)$$

$$\begin{aligned} V_{pcc}^* &= f(V_{pcc}^*) \\ &= \sqrt{V_g^2 - (I_d^{ref} X_g)^2} + k_{q_adj} (0.9 - V_{pcc}^*) X_g \end{aligned} \quad (7)$$

Stability Condition:

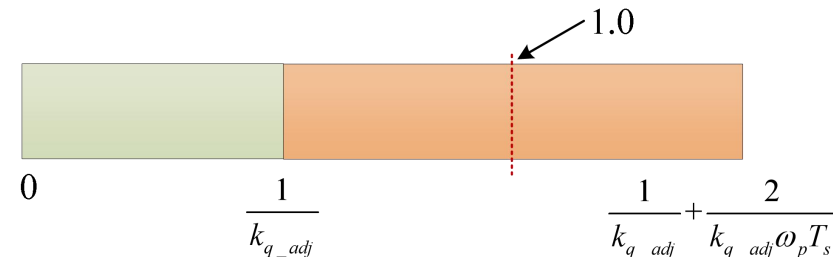
$$\left| \frac{df(V_{pcc}^*)}{dV_{pcc}^*} \right| = k_{q_adj} X_g < 1 \Rightarrow X_g < \frac{1}{k_{q_adj}} \quad (8)$$

The scheme with LPF (the proposed scheme):

$$\begin{aligned} V_{pcc}(n+1) &= \sqrt{V_g^2 - (I_d^{ref} X_g)^2} \\ &+ k_{q_adj} (0.9 - V_{pcc}(n)) * \frac{\omega_p}{\frac{z-1}{zT_s} + \omega_p} X_g \\ &= H - k_{q_adj} X_g V_{pcc}(n) * \frac{\omega_p}{\frac{z-1}{zT_s} + \omega_p} \end{aligned} \quad (9)$$

Stability Condition:

$$\begin{aligned} k_{q_adj} X_g &< \frac{2}{\omega_p T_s} + 1 \\ &\Downarrow \\ X_g &< \frac{1}{k_{q_adj}} + \frac{2}{k_{q_adj} \omega_p T_s} \end{aligned} \quad (10)$$



Verification Results:

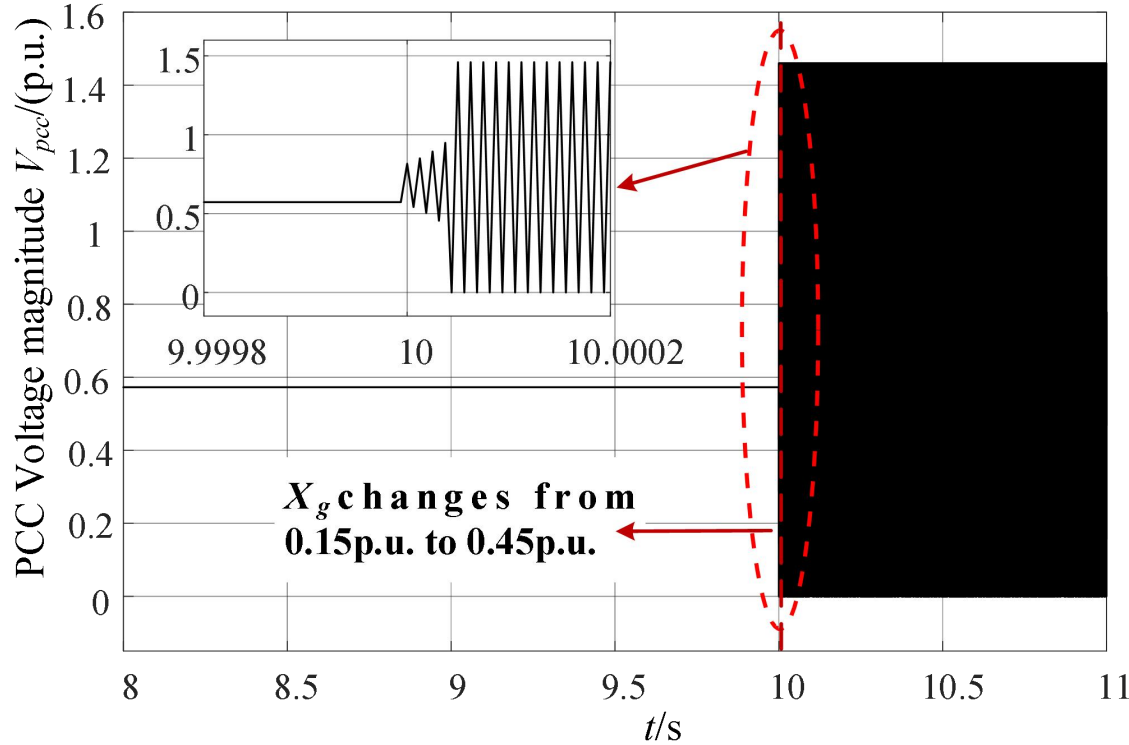


Fig. 7 The PCC voltage of grid-connected inverters during LVRT process when grid impedance changes from 0.15p.u. to 0.45p.u. and the adjustment coefficient of reactive current k_{qadj} keeps as 2.5.

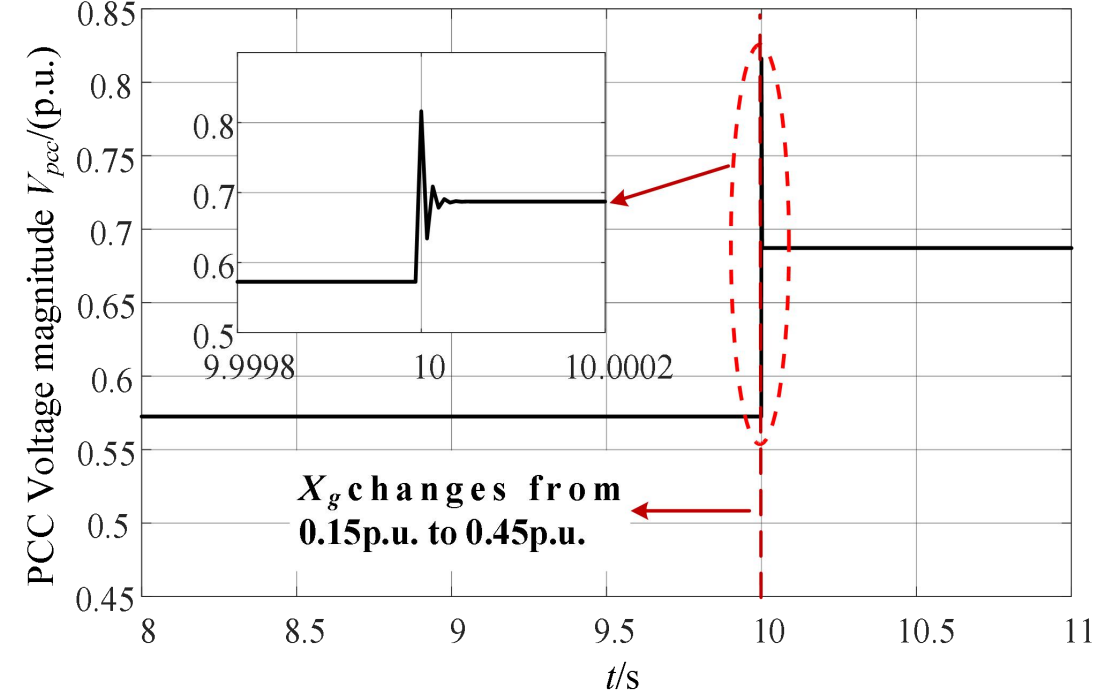
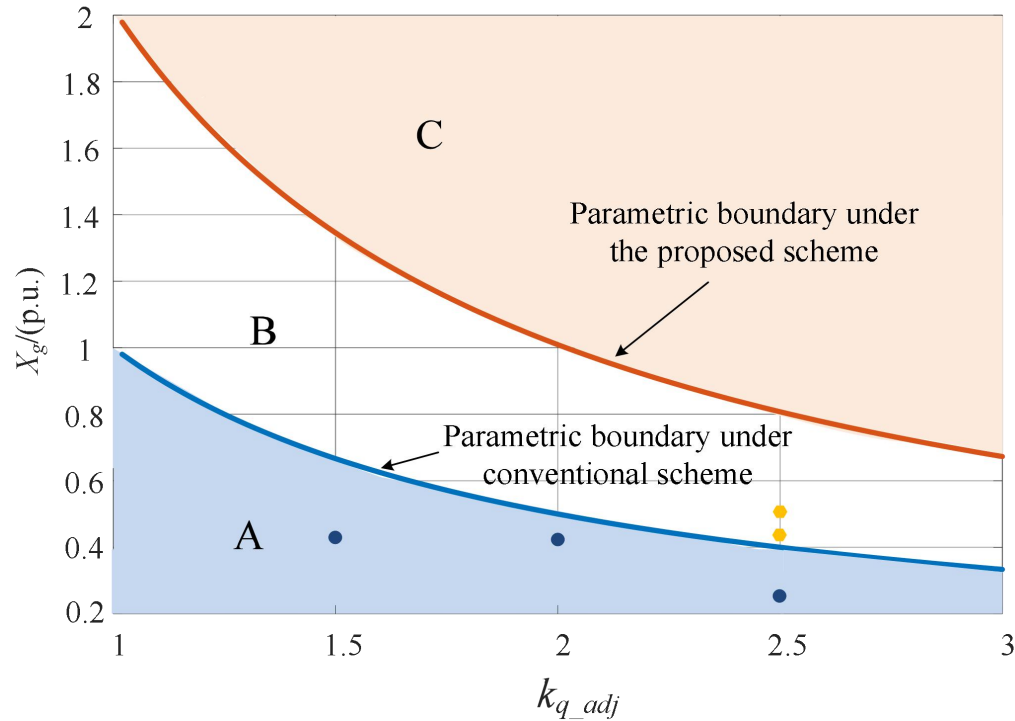


Fig. 10 The PCC voltage of grid-connected inverters during LVRT process when grid impedance changes from 0.15p.u. to 0.45p.u. and the adjustment coefficient of reactive current k_{qadj} keeps as 2.5 under the proposed scheme.

Verification Results:



A whole parametric boundary under the conventional scheme and the proposed scheme is shown in Fig. 11. The stable parametric range is area A under the conventional scheme. All the cases outside of A will be unstable. Under the proposed scheme, the stable parametric area will expand from A to A+B. All the cases inside this area will be stable. These results verify that the proposed scheme can enhance the stability of the inverters.

Fig. 11 The change of the parametric boundary under the conventional scheme and the proposed scheme (● represents the cases after verification).

Conclusions:

An instability phenomenon of grid-connected in-verters caused by the large grid impedance is re-vealed and analyzed. The obtained verification re-sults prove that the large impedance will make the characteristic roots move to the outside of the unit circle leading to instability. The proposed LPF used with the PCC voltage detection module can enlarge the configurable range of grid impedance leading to the enhancement of the stability performance.

- [1] R. Rosso, X. Wang, M. Liserre, X. Lu and S. Engelken, “Grid-Forming Converters: Control Approaches, Grid-Synchronization, and Future Trends—A Review,” IEEE Open J. Ind. Appl., vol. 2, pp. 93-109, Apr. 2021.
- [2] X. Wang, F. Blaabjerg and W. Wu, “Modeling and Analysis of Harmonic Stability in an AC Power-Electronics-Based Power System,” IEEE Trans. on Power Electron., vol. 29, no. 12, pp. 6421-6432, Dec. 2014.
- [3] Pan D, Wang X, Liu F , et al. “Transient Stability of Voltage-Source Converters With Grid-Forming Control: A Design-Oriented Study,” IEEE J. Emerg. Select. Topics Power Electron. vol. 8, no. 2, pp. 1019-1033, Oct. 2019.
- [4] F. Blaabjerg, R. Teodorescu, M. Liserre and A. V. Timbus, “Overview of Control and Grid Syn-chronization for Distributed Power Generation Systems,” IEEE Trans. Ind. Electron., vol. 53, no. 5, pp. 1398-1409, Oct. 2006.
- [5] E. Afshari et al., “Control Strategy for Three-Phase Grid-Connected PV Inverters Enabling Current Limitation Under Unbalanced Faults,” IEEE Trans. Ind. Electron., vol. 64, no. 11, pp. 8908-8918, Nov. 2017.
- [6] Kundur, Power System Stability and Control. New York, NY, USA: McGraw-Hill, 1994.
- [7] Teodorescu, Remus, M. Liserre, and P. Rodri-guez. Grid Converters for Photovoltaic and Wind Power Systems. Wiley, 2011.
- [8] IEEE Standard 929. IEEE Recommended Prac-tice for Utility Interface of Photovoltaic (PV) Sys-tems, IEEE: Piscataway, NJ, USA, 2000.
- [9] IEEE Standard 1547. IEEE Standard for Intercon-necting Distributed Resources with Electric Pow-er Systems, IEEE: Piscataway, NJ, USA, 2003.
- [10] Wu H and Wang X. An Adaptive Phase-Locked Loop for the Transient Stability Enhancement of Grid-Connected Voltage Source Converters, 2018 IEEE Energy Conversion Congress and Exposition (ECCE), OR, USA, 2018: 5892-5898.
- [11] The State Administration for Market Regulation of China. Technical requirements for photovoltaic grid-connected inverter: GB/T 37408-2019, 2019.
- [12] The State Administration for Market Regulation Technical regulations for connecting photovoltaic power stations to power systems: GB/T 19964-2012, 2012.